

QUANTUM CAUSALITY

SERGEY M. KOROTAEV AND EVGENIY O. KIKTENKO

Geoelectromagnetic Research Centre of Schmidt Institute of Physics of the Earth, Russian Academy of Sciences, P.O. 30 Troitsk, Moscow Region 142190, Russia

The quantum extension of causal analysis has shown a rich picture of the subsystem causal connections, where the usual intuitive approach is hampered more commonly. The direction of causal connection is determined by the direction of irreversible information flow, and the measure of this connection, called the course of time c_2 , is determined as the velocity of such flow. The absence of causality corresponds to $|c_2| \rightarrow \infty$, accordingly the degree of causal connection is inversely related to c_2 . This formal definition of causality is valid at any time direction. The possibilities of causal analysis have been demonstrated before by series of examples of the two- and three-qubit states. In this paper we consider the new applications. The first one is the application of quantum causal analysis to the asymmetric entangled state under decoherence. Three models of decoherence: dissipation, depolarization and dephasing are studied. For the all models the strength and the direction of induced causality has been computed. It turns out that the decoherence acting along original causality destroys entanglement to a lesser degree than it acting against this causality. The second application is the interaction between a two-level atom and infinite-dimensional quantized mode of a field by Jaynes-Cummings model. An analytical solution of von Neumann equation for different initial states is examined. The field is considered initially to be in thermal mixed state, while atom – sequentially in excited, ground or thermal states. Negativity, mutual information and causal characteristics for different temperatures are computed. It is obtained that for high temperatures distinction between behaviors of different initial states smoothes over and the state turns out to be causal, entangled and “classical” in entropic sense. And the third application is the teleportation (three-particle protocol). Contrintuitively the teleported qubit is not an effect of the original one; it proves the common effect of both two other ones. But at the same time the result of Bell measurement constitutes a cause with respect to every qubits of entangled pair just since moment of their birth. The latter is manifestation of causality in reverse time.

1. Introduction

The causality is one of the universal physical principles. It plays the twofold role. On the one hand, in the problems brought to the sufficient theoretical level, this principle allows selecting of the physically realizable solutions among a plethora of the mathematically admissible ones. It is just the case of relativity theory. On the other hand, the establishment of causal-effect connections in analysis of the complicated systems is the first step to the construction of a phenomena model. In references to the causality principle, usually it does not bear in mind anything except retardation of the effect relative to the cause. With indefinite terms the “cause” and “effect” in the theoretical problems it may lead to the confusions. In the complicated phenomena investigation the rather serious mistakes are possible. It is particularly important for the quantum entangled states. Usually the question about possible reversal of time ordering at quantum correlation through a spacelike interval is avoided presupposing quantum correlation to be causeless. But it is in conflict with the possibility of quantum information transfer.

Although practically the conflict is damped by the fact that for the communication purposes one should use an ancillary classical subluminal channel, recently the problem became relevant in connection with macroscopic entanglement, quantum wormholes, etc. The necessity of formal taking into account of really existing causal connections was felt by many researchers ([1] and references therein). In answer to this challenge the formal method of classical causal analysis was suggested [2]. This method had been successfully applied before to the various experimental problems of classical physics ([3] and references therein). Recently it is also applied to the experiments on macroscopic entanglement [4-8]. But the classical approach to that quantum phenomenon is rather limited. The quantum extension of causal analysis has shown a richer picture of the subsystem causal connections, where the usual intuitive approach is hampered more commonly [9]. The direction of causal connection is determined by the sign of irreversible information flow, and the measure of this connection, called the course of time, is determined as the velocity of such flow. The absence of causality

corresponds to infinite course of time; accordingly the degree of causal connection is inversely related to its value. This formal definition of causality is valid at any time direction. The independence functions used in the causal analysis allow classification of quantum and classical correlations of the subsystems. The possibilities of causal analysis have been demonstrated before by series of examples of the two- and three-qubit states [9-13].

In this paper we consider the new applications. Quantum mechanical development of the causality concept turns out not only possible, but fruitful in many respects, in particular, in solving of problem of entanglement protection under decoherence. Next, the quantum mechanical principle of weak causality (suggested intuitively long ago by Cramer [14] and formalized now in causal analysis) admits availability of the signals in reverse time for the random processes. It helps to understand the teleportation process and opens way to understanding more complicated phenomena.

In Sec. 2 the kernel of quantum causal analysis formalism is reviewed. In Sec. 3 application of causal analysis to the entangled states under different kinds of decoherence is demonstrated. Sec. 4 is dedicated to the analysis of entanglement and causality in interaction of a two-level atom with the field. In Sec. 5 we consider three-particle teleportation protocol at different approaches and reveal causality in reverse time. The general results are summarized in Sec. 6.

2. Kernel of Quantum Causal Analysis

Quantum causal is an extension of classical causal analysis [2] which operates only with classical variables. The essence of causal analysis bases on formalization of usual intuitive “cause” and “effect” concepts from information-wise asymmetry of a process without invoking time relations. The retardation of effect relative to the cause is introduced after their definition as an axiom.

Consider a quantum bipartite state, which characterized by density matrix ρ_{AB} , which consists of two subsystems A and B with the reduced density matrices $\rho_A = Tr_B \rho_{AB}$ and $\rho_B = Tr_A \rho_{AB}$ respectively. From these matrixes we can calculate corresponding von Neumann entropies $S(A)$, $S(B)$ and $S(AB)$ by general formula:

$$S(X) = -Tr[\rho_X \log_2 \rho_X]. \quad (1)$$

Mathematical formalization of causal analysis is founded on a pair of independence functions:

$$i_{B|A} = \frac{S(B|A)}{S(B)}, \quad i_{A|B} = \frac{S(A|B)}{S(A)}, \quad i \in [-1, 1], \quad (2)$$

where $S(B|A) = S(AB) - S(A)$ and $S(A|B) = S(AB) - S(B)$ are conditional entropies. To understand the idea of independence functions let us consider the main demonstrative cases. $i_{B|A} = -1$ (which can be realized only when $i_{A|B} = -1$) means that we have pure entangled state: $S(AB) = 0$, $S(A) = S(B) \neq 0$, that corresponds to maximal quantum correlations between the two subsystems. If $i_{B|A} = 0$ then $S(AB) = S(A)$ and we obtain that state B is one-valued function of state A (notice, that $i_{B|A} = 0$ does not mean that $i_{A|B} = 0$). Therefore in this context we have maximal classical correlations. And in case of $i_{B|A} = 1$, the B is independent of the A . It is worth to mention, that generally $i_{B|A} \neq i_{A|B}$, so the independence functions characterize one-way correlations between two subsystems in contrast to e.g. mutual information:

$$I = S(A) + S(B) - S(AB), \quad (3)$$

this characterizes total two-way correlation between the subsystems.

It is important that for the classical variables $i \in [0, 1]$, that is a result of the classical inequality $S(AB) \geq \max[S(A), S(B)]$. Therefore independence functions can indicate weather the system is “quantum” or “classical” in entropic sense. If at least one $i_{A|B} < 0$ or $i_{B|A} < 0$, then a system should be called quantum. If both $i_{A|B} > 0$ and $i_{B|A} > 0$, then a system should be called classical. The similar definitions, although in other terms, were proposed before in Ref. [15] (there was considered quantum-classical' bipartite state AB , where the A subsystem was quantum with $i_{B|A} < 0$ and the B was classical with $i_{A|B} > 0$).

Causality in our consideration corresponds to inequality $i_{B|A} \neq i_{A|B}$. For the measure of causal connection between subsystems A and B we use $c_2(A, B)$, called the course of time (notation follows Kozyrev's pioneer work on causal mechanics [1]), and derived in [9-11] as the velocity of irreversible information flow:

$$c_2(A, B) = k \frac{(1 - i_{A|B})(1 - i_{B|A})}{i_{A|B} - i_{B|A}}, \quad (4)$$

where $k = \Delta r / \delta t$, Δr is an effective distance between A and B , and δt is a time of brachistochrone evolution [16]. For the orthogonal states:

$$\delta t = \frac{\pi \hbar}{2(\Delta E)_{\max}}, \quad (5)$$

where $(\Delta E)_{\max}$ is a maximal difference between eigenvalues of the Hamiltonian.

The sign of $c_2(A, B)$ is specified by the direction of causal connection: $c_2(A, B) > 0$ means that subsystem A is a cause (information-wise source) and B is an effect (informational-wise sink). $c_2(A, B) < 0$ means that B is a cause and A is an effect ($c_2(A, B) = -c_2(B, A)$). The strength of the causal connection corresponds to absolute value $|c_2(A, B)|$: the stronger is the causality, the greater is asymmetry, the less is $|c_2(A, B)|$. It is noteworthy that e.g. for all the pure entangled states $|c_2(A, B)| \rightarrow \infty$ that totally conform to representation of quantum correlations as causeless and instantaneous. But in the mixed states the independence functions need not be equal, therefore causality can exist.

Cramer was the first to distinguish the principles of strong and weak causality [14]. The strong causality corresponds to usual condition of retardation $\tau_{A \rightarrow B}$ of the effect relative to the cause:

$$\begin{aligned} c_2(A, B) > 0 &\Rightarrow \tau_{A \rightarrow B} > 0, \\ c_2(A, B) < 0 &\Rightarrow \tau_{A \rightarrow B} < 0, \\ |c_2(A, B)| \rightarrow \infty &\Rightarrow \tau_{A \rightarrow B} \rightarrow 0, \end{aligned} \quad (6)$$

Without the axiom (6) we have weak causality, which corresponds only to nonlocal correlations. Even as they occur in reverse time they only relate the unknown states (hence the ‘‘telegraph to the past’’ is impossible). Although it is not very important for the present work scope, note that weak causality admits the extraction of information from the future without well known classical paradoxes. The experimental possibility of detection of such time reversal phenomena was theoretically predicted by Elitzur and Dolev [17] and really proved for the intramolecular teleportation [18] and for the macroscopic

entanglement, [4-8]. And note that we do not use the axiom (6) anywhere in the current paper.

To keep the examples described bellow from becoming too involved; we shall restrict ourselves by calculations of c_2 with accuracy to $k=1$ in Eq. (4), since it does not qualitatively influence on the c_2 behavior [9,10].

3. Decoherence Asymmetry and Causality

3.1. Models

We consider the models of some well known three-qubit entangled symmetric states – GHZ and W ones where causality originally is absent and emerges only as a result of decoherence, and asymmetric CKW one with finite original causality [9, 10]. The measure of quantum causality c_2 is compared to the negativity N as a standard measure of entanglement.

So, the model states are:

1. Greenberg- Horn-Zeilinger (GHZ) state:

$$|GHZ\rangle = \frac{1}{\sqrt{2}}(|000\rangle + |111\rangle), \quad (7)$$

2. W-state:

$$|W\rangle = \frac{1}{\sqrt{3}}(|001\rangle + |010\rangle + |100\rangle), \quad (8)$$

3. Coffman-Kundu-Wooters (CKW) state [19, 20]:

$$|CKW\rangle = \frac{1}{\sqrt{2}}|100\rangle + \frac{1}{2}(|001\rangle + |010\rangle). \quad (9)$$

The first qubit of every state we call the subsystem A , the second and third ones – the subsystems B and C . Any two-party partitions of (7) and (8) are equivalent. In the state (9) the party A sets off from B and C , therefore only parties B , C and AB , AC are equivalent. Since all the states (7)-(9) are pure any their two-one partitions $AB-C$, $A-BC$, etc. are causeless ($|c_2| \rightarrow \infty$) [9, 10].

Finite causality potentially is possible only in the mixed subsystems $A-B$, $A-C$ and $B-C$. But due to the symmetry there is a finite causality only in the state (9); namely the computations of Ref. [9, 10] has yielded for the state (9): $c_2(A, B) = c_2(A, C) \approx 5.30$. Thus A is the cause with respect to B and C .

The three kinds of decoherence (of $0 \leq p \leq 1$ degree) reduce to the following transformations [21, 22]:

Dissipation:

$$\begin{aligned}
|0\rangle\langle 0| &\rightarrow |0\rangle\langle 0|, \\
|1\rangle\langle 1| &\rightarrow (1-p)|1\rangle\langle 1| + p|0\rangle\langle 0|, \\
|1\rangle\langle 0| &\rightarrow \sqrt{1-p}|1\rangle\langle 0|, \\
|0\rangle\langle 1| &\rightarrow \sqrt{1-p}|0\rangle\langle 1|.
\end{aligned} \tag{10}$$

Depolarization:

$$\begin{aligned}
|0\rangle\langle 0| &\rightarrow (1-p)|0\rangle\langle 0| + p\frac{I}{2}, \\
|1\rangle\langle 1| &\rightarrow (1-p)|1\rangle\langle 1| + p\frac{I}{2}, \\
|1\rangle\langle 0| &\rightarrow (1-p)|1\rangle\langle 0|, \\
|0\rangle\langle 1| &\rightarrow (1-p)|0\rangle\langle 1|.
\end{aligned} \tag{11}$$

Dephasing:

$$\begin{aligned}
|1\rangle\langle 0| &\rightarrow (1-p)|1\rangle\langle 0|, \\
|0\rangle\langle 1| &\rightarrow (1-p)|0\rangle\langle 1|.
\end{aligned} \tag{12}$$

We apply (10)-(12) to one of the qubits of (7)-(9). Due to the symmetry of these states it is enough to apply a transformation to any of qubits of (7) and (8) and we select this qubit to be C . For the state (9) the distinguishable results are achieved by application of a transformation only to the qubits C and A (the transformations of B and C are equivalent).

The resulting mixed states are the following:

Decoherence of GHZ (7):

$$\rho_{GHZ}^{dissC} = \frac{1}{2} \left[\begin{aligned} &|000\rangle\langle 000| + (1-p)|111\rangle\langle 111| \\ &+ p|110\rangle\langle 110| \\ &+ \sqrt{1-p}(|000\rangle\langle 111| + |111\rangle\langle 000|) \end{aligned} \right], \tag{13}$$

$$\rho_{GHZ}^{depolC} = \frac{1}{2} \left[\begin{aligned} &\left(1 - \frac{p}{2}\right) \left(|000\rangle\langle 000| + |000\rangle\langle 111| \right) \\ &+ \left(1 - \frac{p}{2}\right) \left(|111\rangle\langle 000| + |111\rangle\langle 111| \right) \\ &+ \frac{p}{2} \left(|001\rangle\langle 001| + |110\rangle\langle 110| \right), \end{aligned} \right] \tag{14}$$

$$\rho_{GHZ}^{dephC} = \frac{1}{2} \left[\begin{aligned} &|000\rangle\langle 000| + |111\rangle\langle 111| \\ &+ (1-p) \left(|000\rangle\langle 111| + |111\rangle\langle 000| \right) \end{aligned} \right] \tag{15}$$

Decoherence of W (8):

$$\rho_W^{dissC} = \frac{1}{3} \left[\begin{aligned} &|010\rangle\langle 010| + |010\rangle\langle 100| \\ &+ |100\rangle\langle 010| + |100\rangle\langle 100| \\ &+ (1-p)|001\rangle\langle 001| + p|000\rangle\langle 000| \\ &+ \sqrt{1-p} \left(|001\rangle\langle 010| + |001\rangle\langle 100| \right) \\ &+ \sqrt{1-p} \left(|010\rangle\langle 001| + |100\rangle\langle 001| \right) \end{aligned} \right], \tag{16}$$

$$\rho_W^{depolC} = \frac{1}{3} \left[\begin{aligned} &(1-p) \left(|001\rangle\langle 010| + |001\rangle\langle 100| \right) \\ &+ \left(1 - \frac{p}{2}\right) \left(|001\rangle\langle 001| + |010\rangle\langle 010| + |100\rangle\langle 100| \right) \\ &+ \frac{p}{2} \left(|000\rangle\langle 000| + |011\rangle\langle 011| + |011\rangle\langle 101| \right) \\ &+ \frac{p}{2} \left(|101\rangle\langle 011| + |101\rangle\langle 101| \right) \end{aligned} \right], \tag{17}$$

$$\rho_W^{dephC} = \frac{1}{3} \left[\begin{aligned} &|001\rangle\langle 001| + |010\rangle\langle 010| \\ &+ |010\rangle\langle 100| + |100\rangle\langle 010| + |100\rangle\langle 100| \\ &+ (1-p) \left(|001\rangle\langle 010| + |001\rangle\langle 100| \right) \\ &+ (1-p) \left(|010\rangle\langle 001| + |100\rangle\langle 001| \right) \end{aligned} \right]. \tag{18}$$

Decoherence of CKW (9):

$$\rho_{CKW}^{dissC} = \frac{1}{2} \left[\begin{aligned} &\frac{1}{2}|010\rangle\langle 010| + \frac{1}{\sqrt{2}} \left(|010\rangle\langle 100| \right) \\ &+ |100\rangle\langle 100| + \frac{1}{2}(1-p)|001\rangle\langle 001| + \frac{1}{2}p|000\rangle\langle 000| \\ &+ \sqrt{1-p} \left(\frac{1}{2}|001\rangle\langle 010| + \frac{1}{\sqrt{2}}|001\rangle\langle 100| \right) \\ &+ \sqrt{1-p} \left(\frac{1}{2}|010\rangle\langle 001| + \frac{1}{\sqrt{2}}|100\rangle\langle 001| \right) \end{aligned} \right], \tag{19}$$

$$\rho_{CKW}^{depolC} = \frac{1}{2} \left\{ \begin{aligned} &(1-p) \left[\begin{aligned} &\frac{1}{2} \left(|001\rangle\langle 010| \right) \\ &+ \left(|010\rangle\langle 001| + |100\rangle\langle 100| \right) \\ &+ \frac{1}{\sqrt{2}} \left(|001\rangle\langle 100| + |100\rangle\langle 001| \right) \end{aligned} \right] \\ &+ \left(1 - \frac{p}{2}\right) \left[\begin{aligned} &\frac{1}{2} \left(|001\rangle\langle 001| + |010\rangle\langle 010| \right) \\ &+ \frac{1}{\sqrt{2}} \left(|010\rangle\langle 100| + |100\rangle\langle 010| \right) \end{aligned} \right] \end{aligned} \right\} \tag{20}$$

$$+ \frac{p}{2} \left[\begin{aligned} &\frac{1}{2} \left(|000\rangle\langle 000| + |011\rangle\langle 011| \right) \\ &+ \frac{1}{\sqrt{2}} \left(|011\rangle\langle 101| + |101\rangle\langle 011| \right) + |101\rangle\langle 101| \end{aligned} \right],$$

$$\rho_{CKW}^{dephC} = \frac{1}{2} \left\{ \frac{1}{2} (|001\rangle\langle 001| + |010\rangle\langle 010|) + \frac{1}{\sqrt{2}} (|010\rangle\langle 100| + |100\rangle\langle 010|) + |100\rangle\langle 100| \right. \quad (21)$$

$$\left. + \frac{1}{2} (1-p) \left[|001\rangle\langle 010| + |010\rangle\langle 001| + \sqrt{2} (|001\rangle\langle 100| + |100\rangle\langle 001|) \right] \right\};$$

$$\rho_{CKW}^{dissA} = \frac{1}{2} \left[\frac{1}{2} (|001\rangle\langle 001| + |001\rangle\langle 010| + |010\rangle\langle 001| + |010\rangle\langle 010|) + (1-p) |100\rangle\langle 100| + p |000\rangle\langle 000| \right. \quad (22)$$

$$\left. + \sqrt{\frac{1-p}{2}} (|001\rangle\langle 100| + |010\rangle\langle 100| + |100\rangle\langle 001| + |100\rangle\langle 010|) \right];$$

$$\rho_{CKW}^{depolA} = \frac{1}{2} \left\{ \frac{1-p}{\sqrt{2}} (|001\rangle\langle 100| + |010\rangle\langle 100| + |100\rangle\langle 001| + |100\rangle\langle 010|) \right. \quad (23)$$

$$\left. + \left(1 - \frac{p}{2}\right) \left[\frac{1}{2} (|001\rangle\langle 001| + |001\rangle\langle 010| + |010\rangle\langle 001| + |010\rangle\langle 010|) + |100\rangle\langle 100| \right] \right\};$$

$$+ \frac{p}{2} \left[|000\rangle\langle 000| + \frac{1}{2} (|101\rangle\langle 101| + |101\rangle\langle 110| + |110\rangle\langle 101| + |110\rangle\langle 110|) \right];$$

$$\rho_{CKW}^{dephA} = \frac{1}{2} \left[\frac{1}{2} (|001\rangle\langle 001| + |001\rangle\langle 010| + |010\rangle\langle 001| + |010\rangle\langle 010|) + 2|100\rangle\langle 100| \right. \quad (24)$$

$$\left. + \frac{1}{\sqrt{2}} (1-p) (|001\rangle\langle 100| + |010\rangle\langle 100| + |100\rangle\langle 001| + |100\rangle\langle 010|) \right].$$

From Eqs. (13)-(24) we have computed all the marginal and conditional entropies, then – the independence function i like (2), and at last – the course of time c_2 like (4) for all the distinguishable two-party partitions. For the same partitions the negativity N , as a measure of entanglement, has been computed too.

3.2 Causal connections at different kinds of decoherence

Decoherence of the most symmetric GHZ state produces the most simple causality picture shown in Figure 1 (recall that according to our notation $c_2(X, Y) > 0$ means directionality of causal

connection $X \rightarrow Y$, $c_2(X, Y) < 0$ means $Y \rightarrow X$). Only dissipation leads to finite causality in any partition. If the dissipated qubit constitutes an individual party (the partitions $AB-C$ and $B-C$) this party always corresponds to the effect ($c_2(AB, C) > 0$, $c_2(A, C) > 0$) and with the increase of the degree of dissipation p the causality amplifies ($c_2 \rightarrow 0$ at $p \rightarrow 1$). It is in full agreement with the intuitive expectation – the irreversible flow of information is directed to the dissipated particle. The fact that $c_2(AB, C) > c_2(B, C)$ is explained in Ref. [11] by stronger mixedness of the reduced state $\rho(BC)$ as compared to $\rho(ABC)$, because mixedness is a necessary condition of causality. In its turn stronger mixedness of $\rho(BC)$ is the consequence of both interaction with A and dissipation of C i.e. interaction with the non-controlled environment; while mixedness of $\rho(ABC)$ is the consequence of only the latter. Note that in the case of dissipation of one of the particles of two-particle counterpart of GHZ state (that is Bell state) all the corresponding entropies and therefore all the other parameters, including c_2 [9, 10] exactly coincides with those of GHZ $AB-C$ partition. In the partition $AC-B$ the behavior of causality is nontrivial. In contrast to the above case the couple AC including the dissipated particle C constitutes the cause. The fact is dissipation of C decreases $S(C)$ (the states approaches to the certain ground state according to Eq (10)). On the other hand the dissipation of C opens the subsystem AC to the environment and $S(AC)$ increases and has the maximum at $p=1/2$ equal to $3/2$ [11], while $S(B) = const = 1$. The particle B always corresponds to the effect but c_2 is not monotonous: it has the minimum at $p = 0.594$. To explain this fact, note that at $p=0$ the state (13) is pure therefore $c_2(AC, B) \rightarrow \infty$; at $p=1$ the state (11) is maximally mixed, but $S(AC) = S(B)$ (the fully dissipated particle C has “disappeared”) therefore $c_2(AC, B) \rightarrow \infty$ too. The denominator of Eq. (4) for $c_2(AC, B)$: $i_{AC|B} - i_{B|AC}$ has the maximum at $p = 0.401$ [11], while the nominator that is correlation $(1 - i_{AC|B})(1 - i_{B|AC})$ decreases as p increases, therefore $\min c_2$ is shifted to a higher p relative to $1/2$. But by comparison with other partitions causality in the $AC-B$ one is prevailing, as it is seen from Figure 1, at small dissipation ($p < 0.387$).

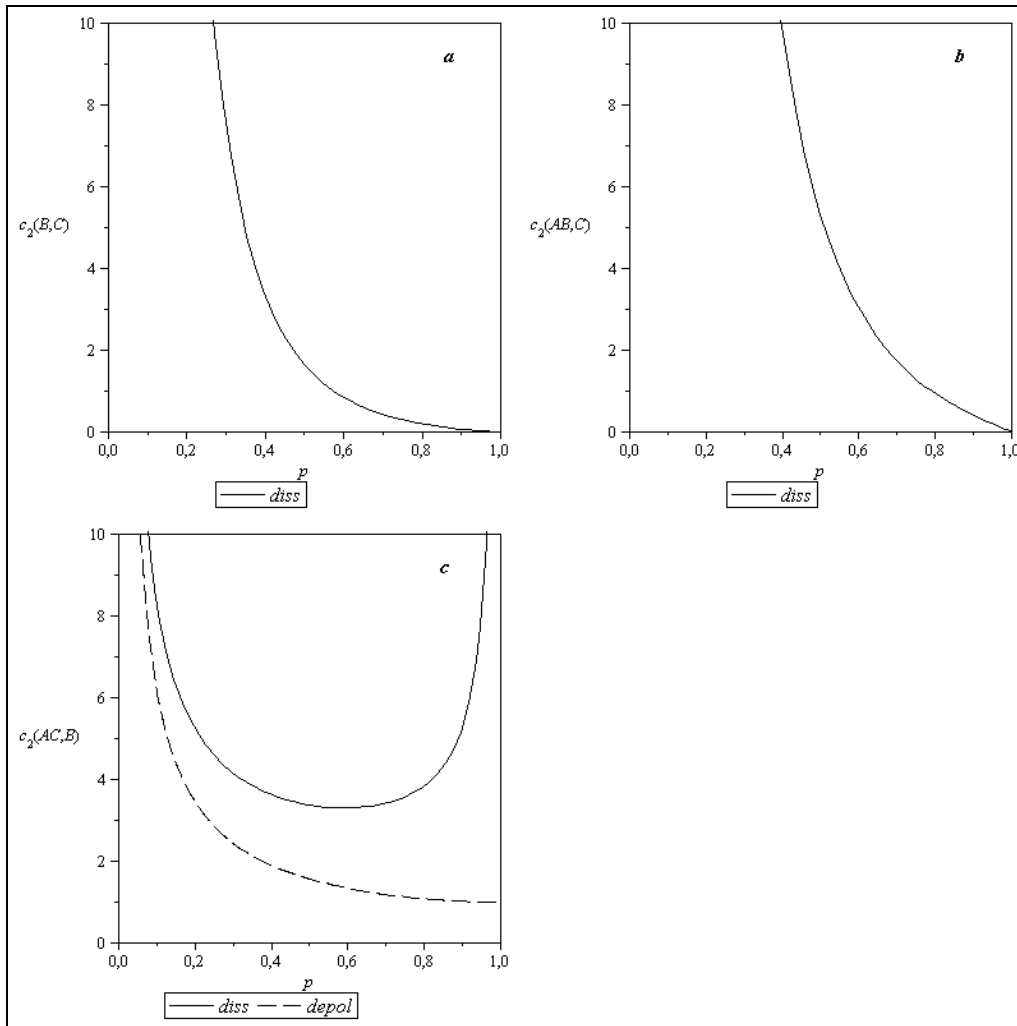


FIGURE 1. Causality in GHZ state with decohered qubit C .

Depolarization leads to only finite causality $AC \rightarrow B$ (Figure 1(c)) that is with the same direction as in the dissipation case but strength of causality amplifies monotonously as p increases, achieving $c_2 = 1$ at $p = 1$.

Dephasing of GHZ state does not lead to emergence of any causality.

W-state decoherence (Figure 2) differs from GHZ one in that depolarization leads to finite causality in all the three partitions, so does the dephasing in $AC - B$ partition. Quantitative features of the c_2 behavior induced by dissipation are the same as in GHZ state and they are explained by the same reasons. The distinction is that c_2 in $AC - B$ partition has the

minimum at $p = 0.576$ and c_2 in this link is higher, i.e. causality is weaker, than in the two other partitions at any p . At depolarization, in contrast to dissipation, if the depolarized qubit constitutes an individual party (the partitions $AB - C$ and $B - C$) this party always is the cause ($c_2(AB, C) < 0$, $c_2(B, C) < 0$) and with the increase of the degree of dissipation p the causality amplifies ($c_2 \rightarrow 0$ at 1). It is also in agreement with the intuitive expectation – the irreversible flow of information (noise) encroaches through the depolarized party and propagates to another one. The fact that $|c_2(AB, C)| > |c_2(B, C)|$ is also explained by stronger mixedness of the reduced state $\rho(BC)$ as compared to $\rho(ABC)$.

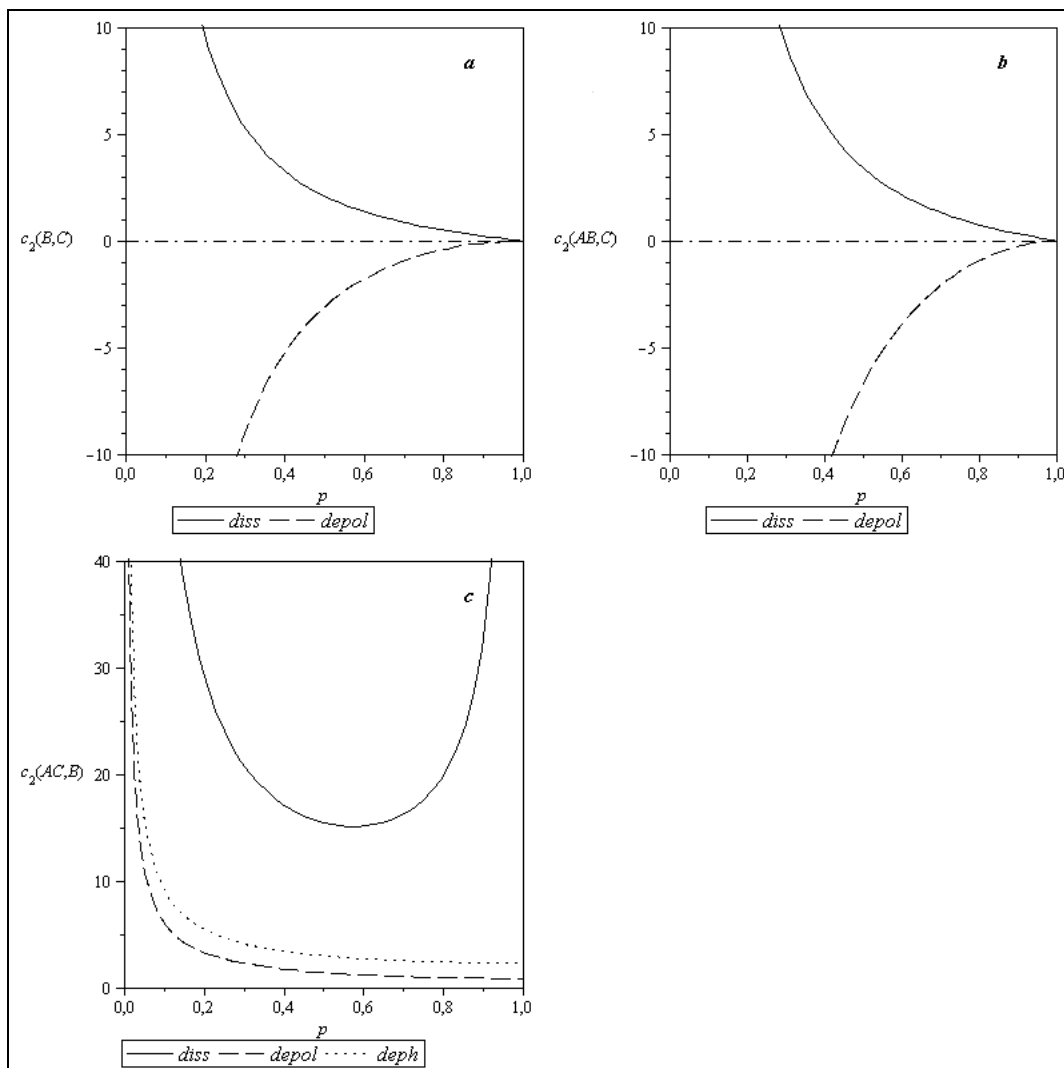
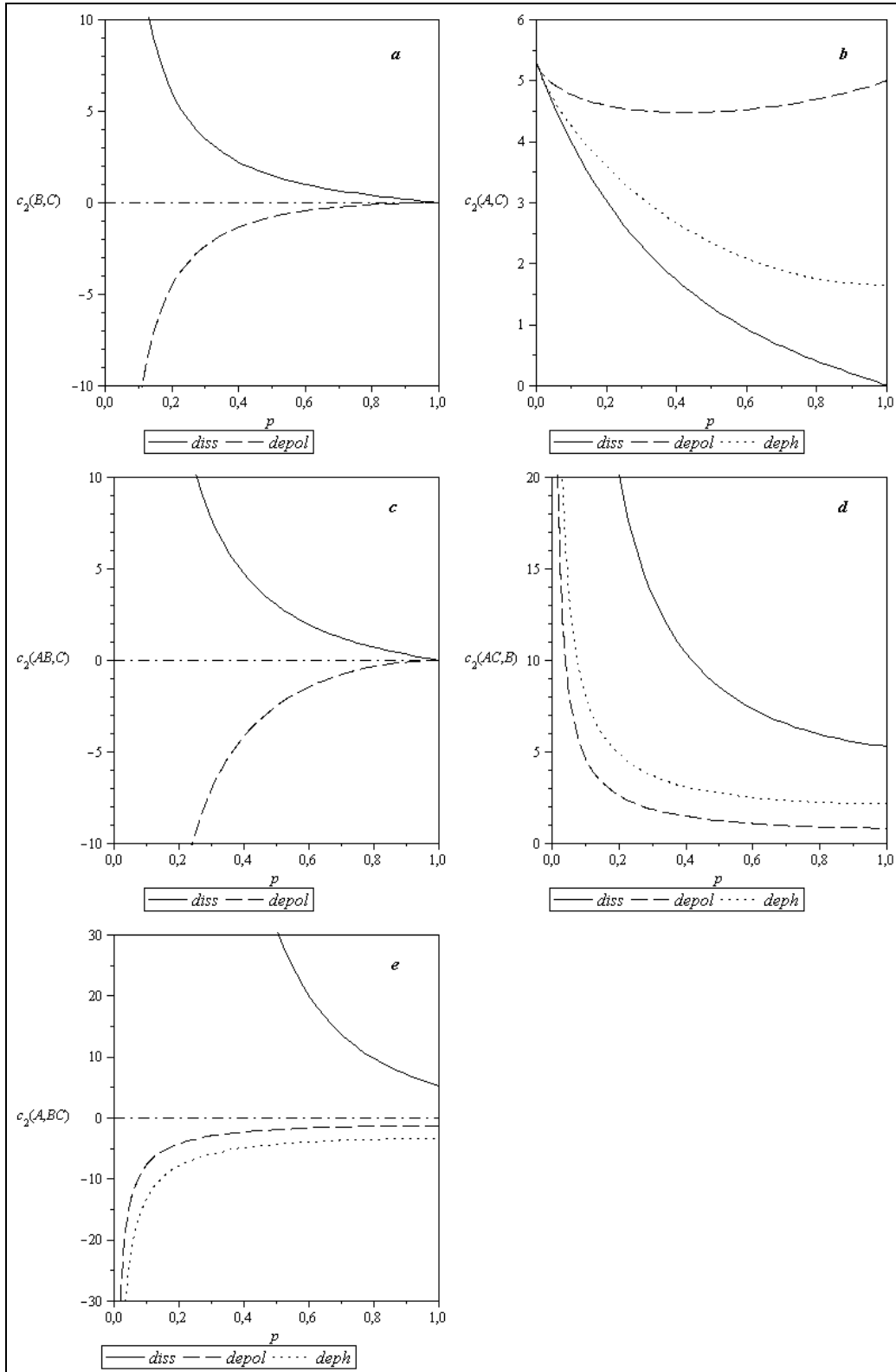


FIGURE 2. Causality in W-state with decohered qubit C .

A comparison between Figures. 1(c) and 2(c) shows that in both the cases directionality of causal connection is $AC \rightarrow B$ and the curves c_2 are alike. In the W-state the dephasing also induces the causality very similar to the depolarization case, but weaker.

The decohered CKW-state, having originally the two causal connections $A \rightarrow B$ and $A \rightarrow C$, produces much more rich induced causality distribution. At the beginning consider an original effect C decoherence (Figure 3).

FIGURE 3. Causality in CKW state with decohered qubit C .

The only pair $B-C$ is originally symmetric and therefore one should expect the same behavior of c_2 as in the W-state. Really Figure 3(a) looks qualitatively like Figure 2(a), but we observe stronger causality at the depolarization. As we have seen before, the depolarization and dissipation, acting on one-qubit party, induce the opposite directions of causal connection with another party. But in the pair $A-C$ (Figure 3(b)) all the three kinds of decoherence amplify the original causality $A \rightarrow C$. The strongest causality is observed in the intuitively expected case of the dissipation. For the depolarization intuitively we could expect reversal or, at least, attenuation of original causality, but it turns out amplified, though nonmonotonously with $\min c_2$ at $p = 0.427$. The reason is that for CKW^C -state $S(A) = 1 = \max$ and it is impossible to reverse causal connection without decreasing $S(A)$ below this maximum. The depolarization of C at relatively small p opens more the subsystem AC and amplifies the original causality. At $p \rightarrow 1$ $S(C)$ increases up to $S(C) = 1 = \max$ and causality returns to its original level.

In the case of partition $AB-C$ (Fig. 3(c)) we have the same as for W-state (Figure 2(b)) and intuitive expected result: the dissipated party C is the effect with respect to AB , whilst the depolarized C is the cause.

If the decohered qubit C is included in the two-qubit party AC (Figure 3(d)) we observe causality $AC \rightarrow B$ at any kind of decoherence. The variation from W-state reduces to the stronger and monotonously amplifying causality at the dissipation. The case of partition $A-BC$ (Figure 3(e)) is close, but at depolarization and dephasing $BC \rightarrow A$, while at dissipation $A \rightarrow BC$. This peculiarity of dissipation is clear. Indeed, at full dissipation ($p = 1$) the particle C “disappears” from its two particle party and as a result $c_2(AC, B) = c_2(A, BC) = c_2(A, B) = 5.30$.

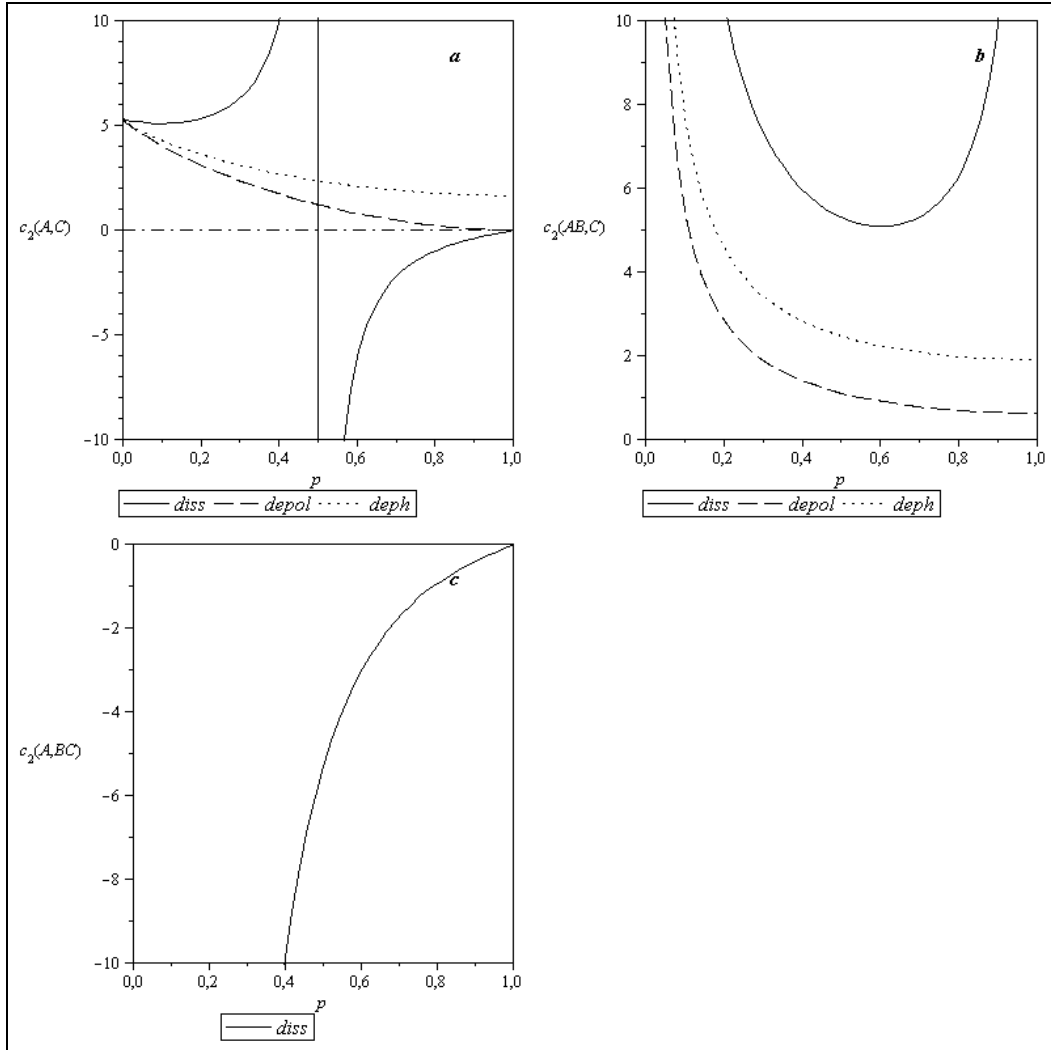
The original cause A decoherence leads to the different causal picture (Figure 4). One may expect that as a result of increasing dissipation of A , the original causal connection $A \rightarrow C$ will at the beginning attenuate until disappearance at some p ,

after that direction of causality will reverse with further utmost amplification of the connection $C \rightarrow A$ as p will tend to 1. In Figure 4(a) it is seen that indeed $c_2(A, C)$ changes its sign at $p = 1/2$. But the variation of positive $c_2(A, C)$ (corresponding to directionality of the causal connection $A \rightarrow C$) proves to be not monotonous; it has the intuitively unexpected minimum equal to 5.08 at $p = 0.103$. Next, in the pair $A-C$ (Figure 4(a)) the depolarization leads to considerable and monotonous amplification of causality as compared to CKW^C (Figure 3(b)). On the one hand, it is in agreement with intuition (the depolarized A becomes the more intensive information source). On the other hand, it can easily be shown that $S(A)$ and $S(C)$ remain independent of p , which demonstrates that one should not consider the marginal entropic asymmetry as a sufficient condition or measure of causality.

In the partition $AB-C$ (Figure 4(b)) the directionality of causal connection is $AB \rightarrow C$ at any kind of decoherence, therewith the c_2 curves for depolarization and dephasing are monotonous like Figure 3(c), while for dissipation the curve has the minimum at $p = 0.603$. The reason of this curve tends to infinity at $p \rightarrow 1$ is that at full dissipation the partition $AB-C$ becomes equivalent to the symmetric one $B-C$. It is notable that at dissipation $\min c_2(AB, C) = \min c_2(A, C)$. And there is an interesting relation, which is valid not only in this model [13]:

$$p(\min c_2(AC, B)) = 1 - p(|c_2(A, C)| = \infty) + p(\min c_2(A, C)).$$

In contrast to the case when the decohered single-party was the original effect C (Figure 3(c)), in the case of decoherence of the original cause A (Figure 4(c)) only dissipation induces the causal connection, therewith A becomes the effect. The monotonous increase of negative $c_2(A, BC)$ simply reflects amplification of causality along with increase of dissipation of the effect A . At the same time $|c_2(AB, C^{diss})| \rightarrow 0$ at $p \rightarrow 1$ quicker than $|c_2(A^{diss}, BC)|$. It reflects the influence of the original (at $p = 0$) causality $A \rightarrow C$.

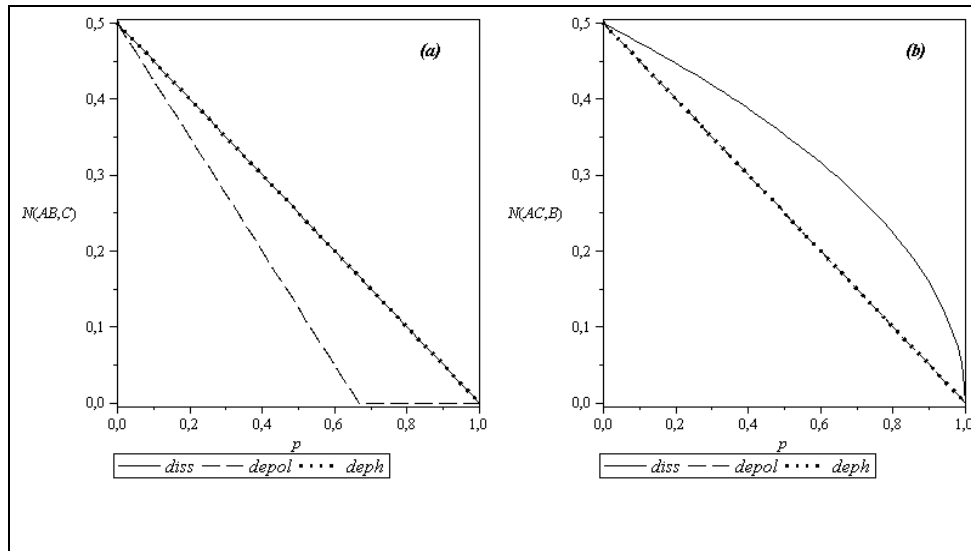
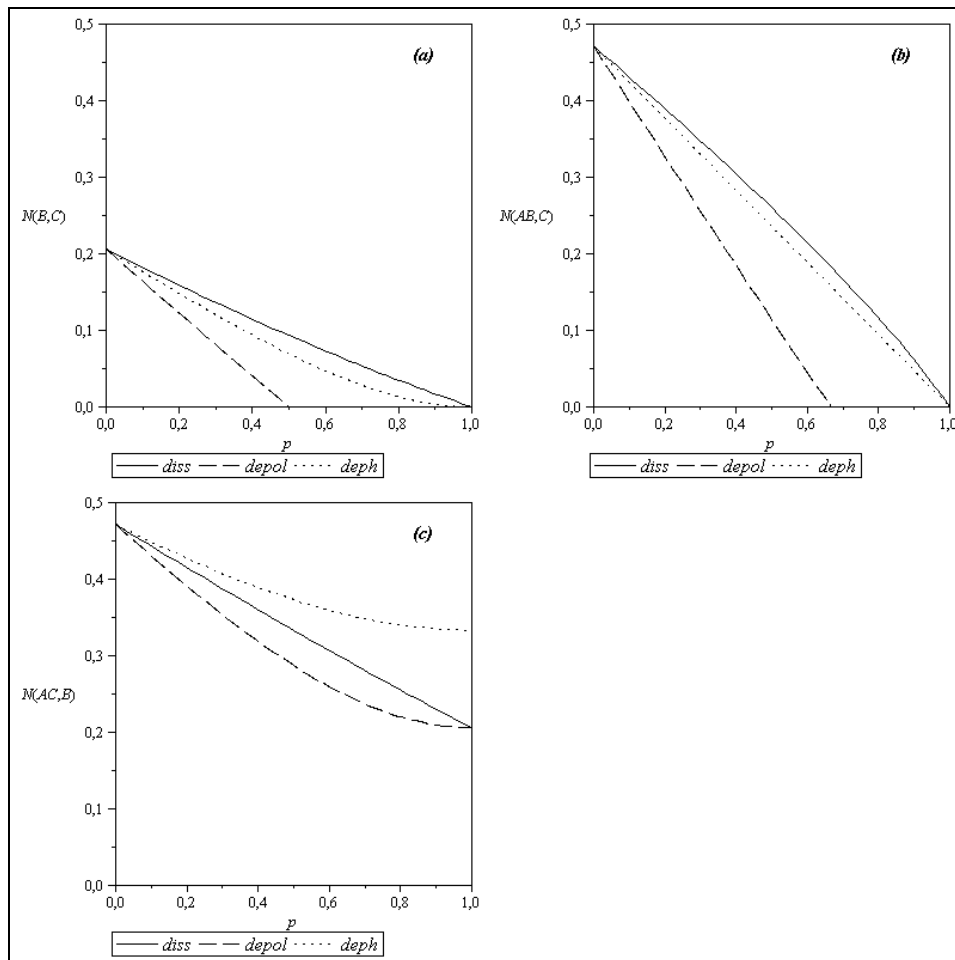
FIGURE 4. Causality in CKW state with decohered qubit A .

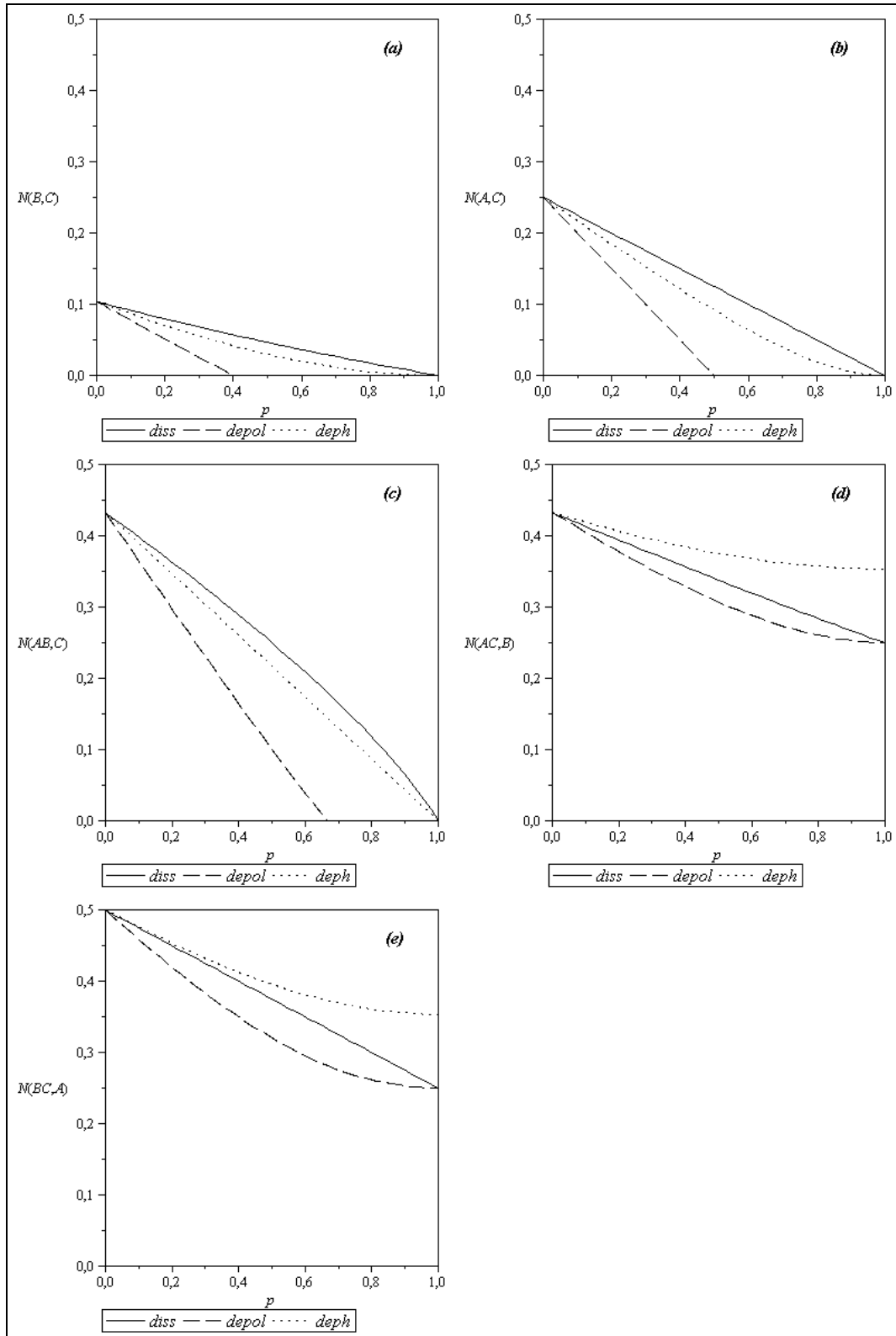
3.3 Relation between entanglement decay and causality

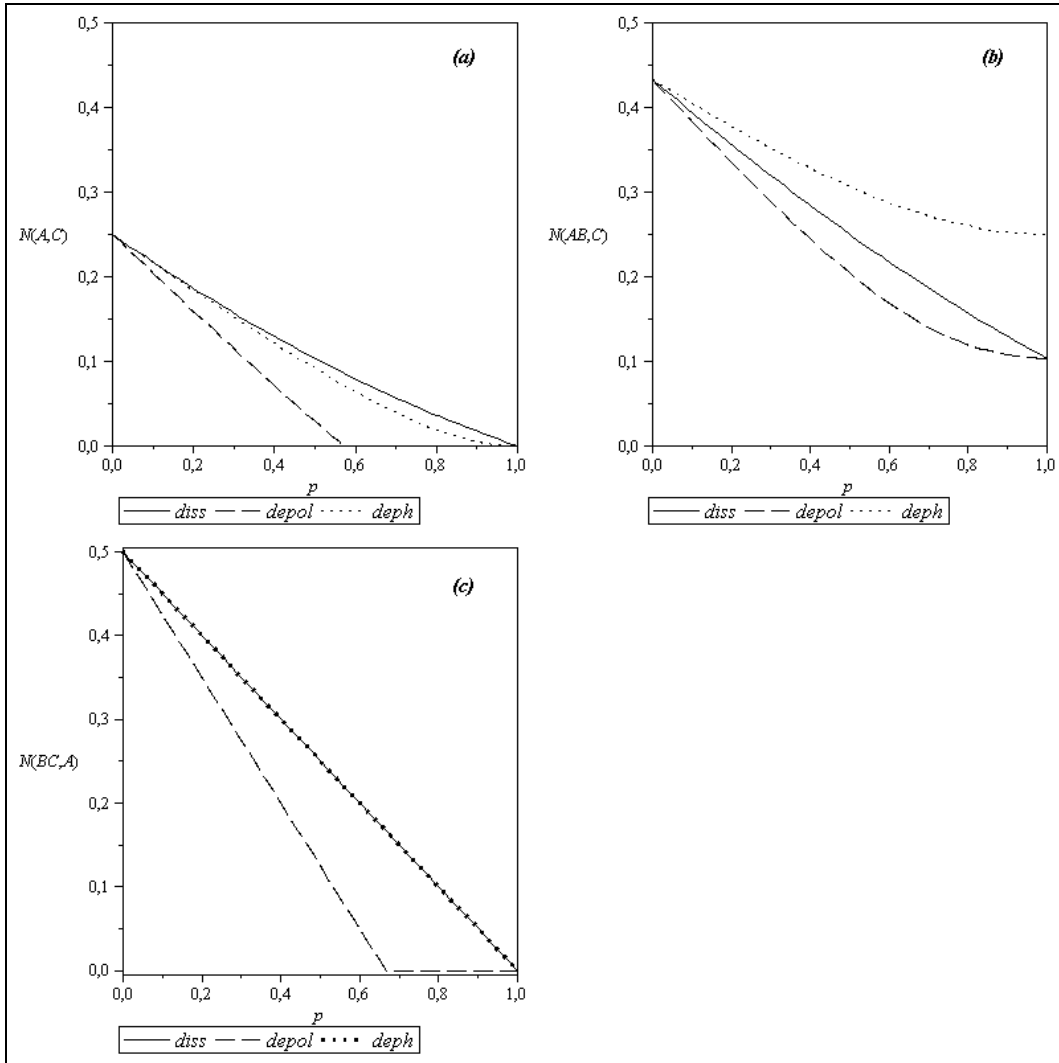
All the considered states in any partition (except pairwise one in GHZ state) are entangled. Compare decrease of negativity N with increasing p presented in Figures 5-8 with c_2 variation in corresponding Figures 1-4.

If we compare N in accordance to whether the decohered party is a cause or an effect within a given state, we conclude that almost always (except GHZ $AB-C$) $N(\text{cause}) < N(\text{effect})$. Further if we compare decoherence of the causes (within a given state) with different values of c_2 , we conclude that decoherence in the cases of lesser c_2 (stronger

causality) leads to the stronger decrease of N . The inverse conclusion follows from comparison of decoherence of the effect with different values of c_2 . Apparently we obtain a quite logical conclusion: the cause decoherence leads to more dramatic decay of entanglement than the effect one and the stronger causality the stronger decay. That is causality reveals the role of asymmetry in information propagation (harmful for entanglement in this context). But in this consideration we have to compare the different kinds of decoherence. Such a consideration can not distinguish the role of causality and decoherence manner.

FIGURE 5. Negativity of GHZ state with decohered qubit C .FIGURE 6. Negativity of W-state with decohered qubit C .

FIGURE 7. Negativity of CKW state with decohered qubit C .

FIGURE 8. Negativity of CKW state with decohered qubit A .

Another approach is the comparison of N and c_2 at fixed both the state and the kind of decoherence. Therefore we should consider the original cause decoherence (A) and effect (C) in CKW state.

Begin with the reduced states. Therewith the case of dephasing is irrelevant ($N^{dephC} = N^{dephA}$). In the dissipated CKW state (Figures 7(b) and 8(a)) $N^{dissC} > N^{dissA}$. As we already know, dissipation of A leads to reversal of original causality (Figure 4(a)); dissipation of C amplifies original causality (Figure 3(b): $|c_2(A, dissC)| < |c_2(dissA, C)|$). We conclude that dissipation, amplifying original causality, destroys entanglement to a lower extent than dissipation, acting against it.

In the depolarized CKW state (Figures 7(b) and 8(a)) $N^{depolC} < N^{depolA}$. And we know that depolarization of A leads to the strong amplification of the original causality (Figure 4(a); depolarization of C only slightly varies it (Figure 3(b): $|c_2(A, depolC)| > |c_2(depolA, C)|$). We conclude that depolarization, amplifying original causality, destroys entanglement to a lower extent than depolarization, acting almost indifferently or against it.

Both the conclusions coincide. Decoherence by the dissipation or depolarization acting along original causality is better from viewpoint of entanglement persistence, than acting against this causality. In other words, for entanglement persistence one should not

“stroke the system against the grain”. As a consequence, having compared the above inequalities for N and c_2 , we infer that stronger entanglement corresponds to stronger causality. Of course, this inference is not universal, but it shows that less information-wise symmetric states can be more entangled.

Now consider decoherence in the partitions where a decohered qubit is in the party AC (or AB). That is the party consists of both the original cause and effect. Thus we consider influence of the “internal” causality variation on entanglement in the partition $AC-B$ in CKW state. The corresponding curves of Figures 7(c) and 8(b) evidence at any of three ways of decoherence at any fixed p : $N^{decohC} > N^{decohA}$. The inference is nontrivial: the decohered internal effect destroys entanglement to a lower extent than the decohered internal cause.

4. Entanglement and Causality in Interaction of a Two-level Atom with the Field

4.1 Interaction model

We consider a bipartite system which consists of a two-level atom, which can be founded in the ground state $|g\rangle_a$ and excited state $|e\rangle_a$, and quantized mode of a field with possible energy states $|0\rangle_f, |1\rangle_f, |2\rangle_f, \dots$. For simplification we set detuning frequency to zero (resonance case is considered). The interaction is described by Jaynes-Cummings model (JCM) with the Hamiltonian:

$$H = \frac{1}{2}\hbar\omega\sigma_z + \hbar\omega a_f^\dagger a_f + \hbar g(|e\rangle_a \langle g|_a a_f + |g\rangle_a \langle e|_a a_f^\dagger), \quad (25)$$

where ω is the resonance frequency, a_f^\dagger and a_f are the creation and annihilation operators respectively, g is dipole matrix element which determines Rabi frequency. It is helpful to write the Hamiltonian of the full system as a sum of two commuting parts: $H = H_0 + V$, where $H_0 = \frac{1}{2}\hbar\omega\sigma_z + \hbar\omega a_f^\dagger a_f$ is diagonal matrix and $V = \hbar g(|e\rangle_a \langle g|_a a_f + |g\rangle_a \langle e|_a a_f^\dagger)$ is matrix with only off diagonal elements and corresponds to the interaction between the subsystems.

The dynamics of the system is described by von Neumann equation:

$$i\hbar \frac{\partial \rho_{af}(t)}{\partial t} = [H, \rho_{af}(t)], \quad (26)$$

where $\rho_{af}(t)$ is a density matrix of whole system. The Hamiltonian (25) is time independent, the solution of (26) is:

$$\rho_{af}(t) = e^{-iHt/\hbar} \rho_{af}(0) e^{iHt/\hbar}, \quad (27)$$

If the initial state is diagonal (later we will see that such is the case) then $e^{-iHt/\hbar} \rho_{af}(0) e^{iHt/\hbar} = \rho_{af}(0)$, so the resulting solution of Eq. (26) takes the form

$$\rho_{af}(t) = e^{-iVt/\hbar} \rho_{af}(0) e^{iVt/\hbar}. \quad (28)$$

In our consideration we deal only with separable initial states:

$$\rho_{af}(0) = \rho_a(0) \otimes \rho_f(0), \quad (29)$$

where $\rho_a(0)$ and $\rho_f(0)$ are the initial states of atom and field respectively.

In the all variants we consider field initially to be in the mixed thermal state

$$\rho_f(0) = \sum_{i=1}^{\infty} P_i |i\rangle \langle i|_f, \quad (30)$$

where P_i is the probability distribution. As the field satisfies Bose-Einstein statistics, we have

$$P_i = \frac{1}{1 + \langle n \rangle} \left(\frac{\langle n \rangle}{1 + \langle n \rangle} \right)^i, \quad (31)$$

with the mean photon number

$$\langle n \rangle = \frac{1}{e^{\hbar\omega/k_B T} - 1}, \quad (32)$$

where T is the temperature. As we see $\langle n \rangle$ characterizes the temperature of the field.

Next one should examine a computational problems caused by infinite dimensionality of $\rho_a(0)$. It is evident from Eq. (31) P_i are exponentially decaying series so that contribution of the matrix elements $P_i |i\rangle \langle i|_f$ at sufficiently high i vanishes. Therefore we can confine series P_i at $i = N_{\max} - 1$ and estimate occurred error as

$$\varepsilon = 1 - \sum_{i=0}^{N_{\max}-1} P_i = \left[\langle n \rangle / (1 + \langle n \rangle) \right]^{N_{\max}}. \quad (33)$$

For our calculations we have set $N_{\max} = 400$, which gives $\varepsilon = 0.007 < 1\%$ at the highest $\langle n \rangle = 80$. At lower $\langle n \rangle$ calculations are much more accurate.

For the initial states of an atom $\rho_a(0)$ we consider the pure excited and ground states:

$$\rho_{af}^e(0) = |e\rangle\langle e|_a \otimes \rho_f(0), \quad (34)$$

$$\rho_{af}^g(0) = |g\rangle\langle g|_a \otimes \rho_f(0). \quad (35)$$

Finally these states give two different solutions of Eq. (28), which we will discuss further.

4.2. Computation results

With the density matrix $\rho_{af}(t)$ we can compute the reduced matrices of atom and field: $\rho_a(t) = Tr_f \rho_{af}(t)$ and $\rho_f(t) = Tr_a \rho_{af}(t)$. From these three matrices we can get time dependent von Neumann entropies of the whole system $S(af)$ and the two subsystems $S(a)$ and $S(f)$ by Eq. (1). Then we can compute the mutual information (3) and the independence functions $i_{a|f}$ and $i_{f|a}$ (2), which determine the course of time (4). As we shall see further, it turns out

$i_{f|a} > i_{a|f}$, so in our consideration we use the notation $c_2(f, a)$ to deal with the positive values. And like before, we use the negativity N as a measure of entanglement.

Let us start the overview of computation results from the initial state (34), where the atom is in the pure excited state and the field is in the thermal mixed state. At $\langle n \rangle = 0$ we get the pure oscillating entangled state vector $|\psi_{af}^e\rangle = \sin(t)|g, 1\rangle_{af} - i \cos(t)|e, 0\rangle_{af}$. Because of whole state purity we have $i_{a|f} = i_{a|f} = -1$ and $c_2(f, a) = \infty$.

In Figure 9(a) the dynamics of negativity for $\langle n \rangle = 0$, $\langle n \rangle = 1$ and $\langle n \rangle = 10$ is presented. As we see, the range of N variations decays and negativity begins to fluctuate near the average value. Moreover, the entanglement is present at $\langle n \rangle > 0$ and $t > 0$ in total agreement with results of Ref. [23].

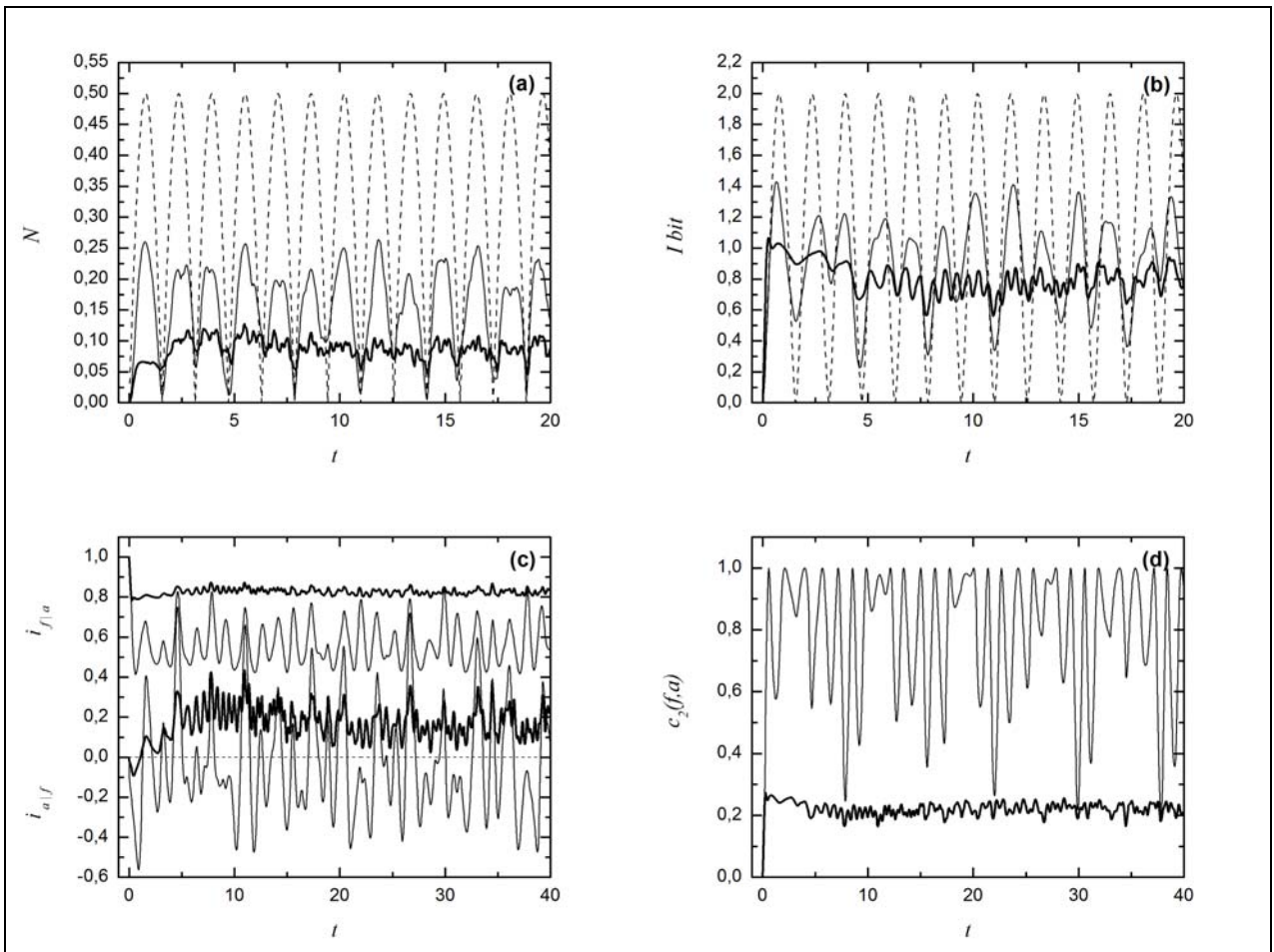


FIGURE 9. Dynamics of characteristics for the initial state (34) at $\langle n \rangle = 1$ (thin lines) and $\langle n \rangle = 10$ (bold lines): (a) negativity (dashed line corresponds to $\langle n \rangle = 0$); (b) information; (c) independence functions $i_{f|a}$ (upper lines) and $i_{a|f}$ (lower lines); (d) causality.

The same behavior shows mutual information I in Figure 9(b), which corresponds to total correlations between the subsystems. It also decays with temperature growth and again it is positive at all times except $t = 0$ (at nonzero temperature).

More detailed description of correlations independence functions present, which are shown in Figure 9(c). As we see $i_{f|a} > i_{a|f}$, so our system is asymmetric and the field corresponds to the cause (information source) and the atom corresponds to the effect (informational sink). Also it is very interesting, that in contrast to case $\langle n \rangle = 1$, when our system demonstrates quantum properties ($i_{a|f}$ can be negative), at $\langle n \rangle = 10$ both independence functions remain positive at t greater than about 1. It means that system is classical in entropic sense but still is entangled. Causality is presented in Figure 9(d). It is

particularly remarkable that that for $\langle n \rangle = 1$ $c_2(f, a)$ is bounded by unit value. With temperature increase the variation and average value of $c_2(f, a)$ decrease, so we see amplification of the causal connection.

It also notable that time of transfer to quasistationary state grows with the temperature rise (the most demonstrable is Figure 9(c). After this time all the characteristics of the system begin to fluctuate near some average values. The extent of such fluctuations goes down with the temperature increase.

Next consider the case of initial state (35), where an atom is in the ground state, while the field still is in the thermal state (Figure 10). At $\langle n \rangle = 0$ we have stationary separable state vector $|\psi_{af}^g\rangle = |g, 0\rangle_{af} = const$, which is classically uncorrelated too: $i_{a|f} = i_{f|a} = 1$.

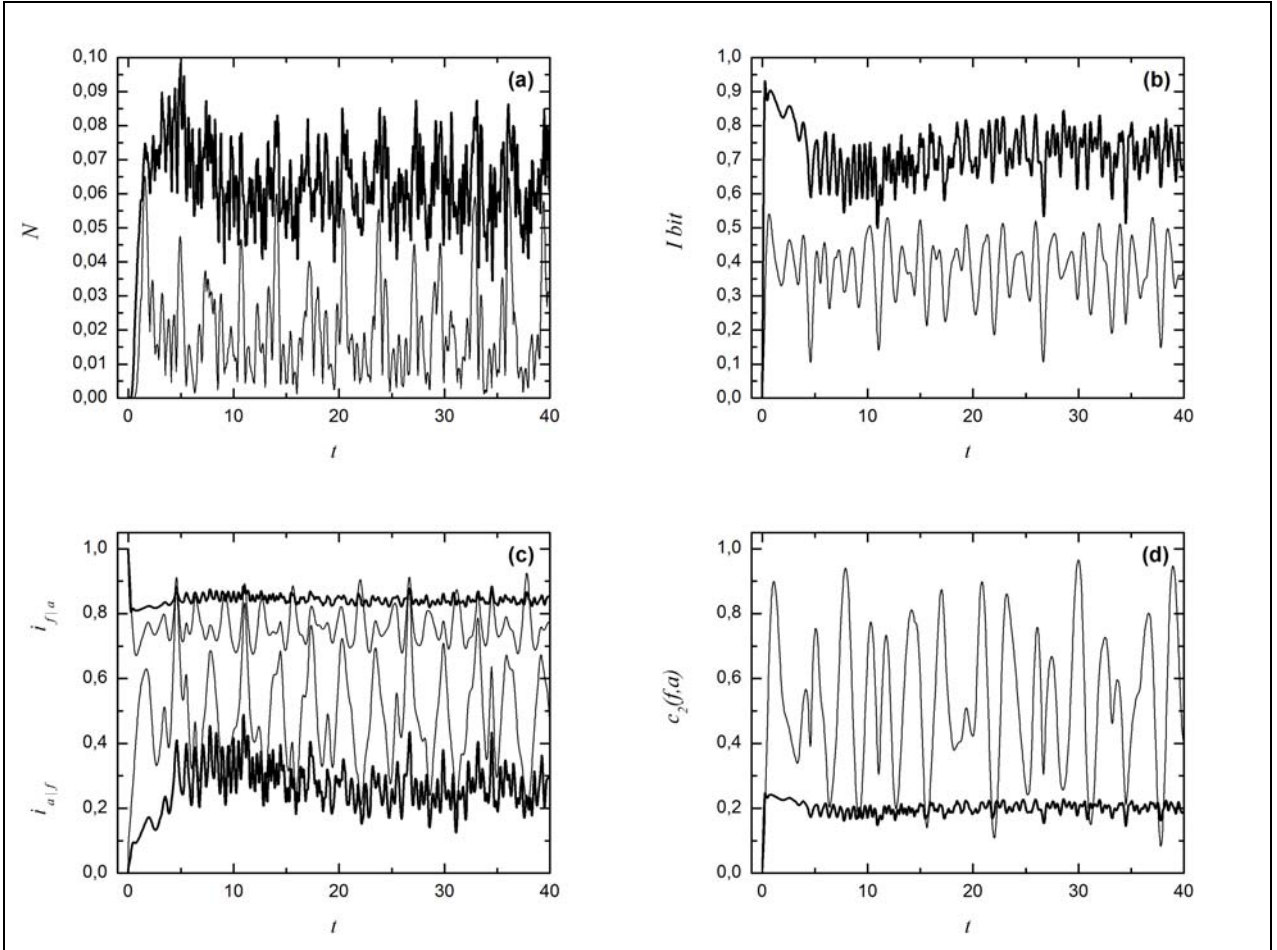


FIGURE 10. Dynamics of characteristics for the initial state (35) at $\langle n \rangle = 1$ (thin lines) and $\langle n \rangle = 10$ (bold lines): (a) negativity; (b) information; (c) independence functions $i_{f|a}$ (upper lines) and $i_{a|f}$ (lower lines); (d) causality.

As it is seen from Figure 10(a) with a rise of $\langle n \rangle$ there is an increase of the negativity: the atom in the ground state becomes entangled with nonzero energy states of the field ($|1\rangle_f, |2\rangle_f, \dots$). The same behavior demonstrates information in Figure 10(b). It might be presupposed (as the temperature is held to have a destructive influence on correlations) that there is some $\langle n \rangle$ after which an entanglement and information would decrease. But it is not the case. The independence functions in Figure 10(c) show that system always is classical in entropic sense. And again the independence functions demonstrate asymmetry between the subsystems: $i_{f|a} > i_{a|f}$ (the field state still is the cause with respect to the atom state. Causality is presented in Figure 10 (d). As well as in previous case it amplifies with the temperature increase.

As we have seen, all parameters of the system for both considered initial states fluctuate near some average values at high temperatures. It seems logically to estimate these values as functions of $\langle n \rangle$. We have chosen time series $150 \leq t \leq 400$ with time step $dt = 0.5$ and have computed the average values $N_{av}, I_{av}, i_{f|a(av)}, i_{a|f(av)}, c_{2(av)}$ for the set of mean photon numbers $1 \leq \langle n \rangle \leq 80$. $t_{min} = 150$ has been chosen to avoid getting in time of transfer to quasistationary state it is high enough for our biggest $\langle n \rangle = 80$. Time step $dt = 0.5$ has been chosen as it does not correspond to any of system eigenfrequencies. Also with average values we have stored minimal and maximal values of characteristics to see variability at our time series. The results of such time averaging are presented in Figure 11.

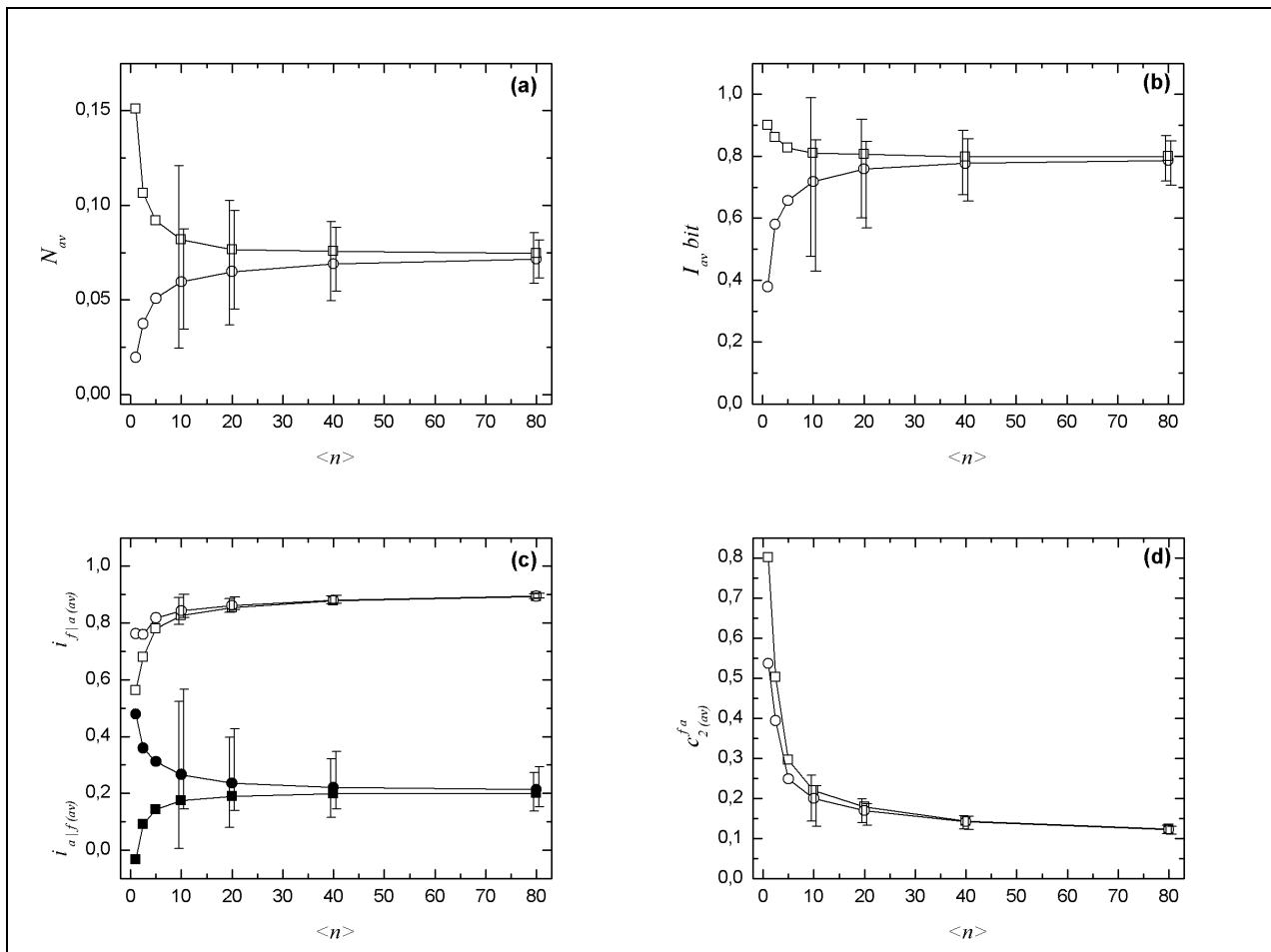


FIGURE 11. Time averaged characteristics and corresponding minimal and maximal values as functions of $\langle n \rangle$ for different initial states: squares and right vertical lines (34), circles and middle vertical lines (35). Averaged characteristics: (a) negativity; (b) information; (c) independence functions $i_{f|a}$ (empty symbols) and $i_{a|f}$ (filled symbols); (d) causality.

First, let us discuss the general features. As noted above the extent of fluctuation for all the parameters decreases with the temperature growth. Moreover the distance between the curves for different initial states decreases: it means that the significance of atom initial states for the average characteristics disappears at the high temperature. It totally corresponds to the result that field is an information source that is a cause.

The most interesting is Figure 11 (a), which demonstrates dependence of negativity on $\langle n \rangle$. It is expectable that for initially pure excited state of the atom entanglement decreases with the temperature rise, but it surprisingly does not vanish. It tends to an asymptotic value, as well as the curve for the initially ground state. It is intriguing that for the ground initial atom state there is an amplification of entanglement with growth of the temperature, so in this case the temperature creates entanglement.

All the other characteristics also have such asymptotic values, as it is seen in Fig. 11(b)-(d). We can estimate that for $\langle n \rangle \gg 1$ the averaged values are: $N_{av} \approx 0.07$ (14% of maximal value), $I_{av} \approx 0.8 \text{ bit}$, $i_{a|f(av)} \approx 0.90$, $i_{f|a} \approx 0.25$, $c_2(f, a)_{av} \approx 0.25$ – the field state is the cause with respect to the atom state.

We can summarize the time averaged results (Figure 11) as follows. Information, reflecting total correlations behaves similarly to the negativity. But the independence functions are completely positive that is classical. The atom-field state is entangled, but correlations are apparently classical. The field state is the cause with respect to the atom one under any conditions. However relation between the degrees of causality and entanglement at the low temperature strongly depends on the initial conditions. At the high temperature both causality and entanglement are indifferent to them.

5. Teleportation

Teleportation is well known and amazing quantum phenomenon. The most interesting fact is that teleportation protocol can be considered as a process involving hidden signal transmission in reverse time. And it does not turn out a matter of “sophisticated” interpretation. The experiment based on postselection gave a direct proof of such a time reversal [18]. Another experiment demonstrated the possibility of teleportation traveling along closed time-like curve without the classical paradoxes [24]. At last, recently

the experiment on entanglement swapping (that is teleportation of entanglement) has demonstrated, even without postselection, quantum information transfer from the future to the past; in fact it has demonstrated a possibility of observation of the random future as the existing reality [25]. Thus teleportation is just such a process where determination of causality irrespective to time direction is relevant.

We consider the standard three-particle (three-qubit) teleportation protocol (Figure 12).

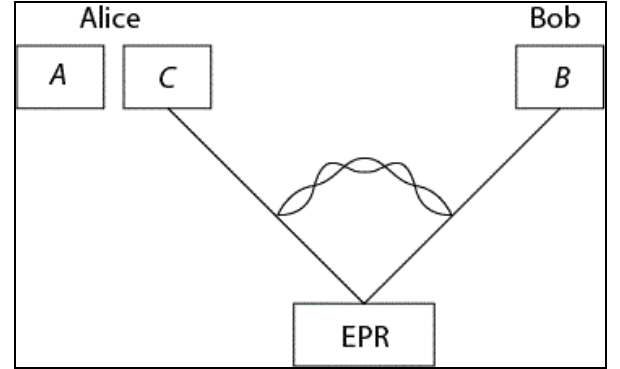


FIGURE 12. Qubit A teleports onto qubit B .

The input particle, which state to be teleported by Alice, is A ; the EPR source produces two entangled particles in the state

$$|\Psi^-\rangle_{BC} = \frac{1}{\sqrt{2}}(|01\rangle - |10\rangle), \quad (36)$$

one of which, B goes to Bob, another one, C goes to Alice, who performs Bell measurement with four possible outcomes:

$$|\Phi^+\rangle_{AC} = \frac{1}{\sqrt{2}}(|00\rangle + |11\rangle). \quad (40)$$

$$|\Phi^-\rangle_{AC} = \frac{1}{\sqrt{2}}(|00\rangle - |11\rangle), \quad (39)$$

$$|\Psi^+\rangle_{AC} = \frac{1}{\sqrt{2}}(|01\rangle + |10\rangle), \quad (38)$$

$$|\Psi^-\rangle_{AC} = \frac{1}{\sqrt{2}}(|01\rangle - |10\rangle), \quad (37)$$

If her result is (40) the output state B coincides with input A , if not – Bob performs a unitary operation on B to complete the protocol. In any case Bob needs information about Alice result, which she sends him

through an ancillary classical channel. As we are interested in investigation of quantum information namely, we exclude this channel. Instead Bob may measure his particle B . Note that any measurement (by Alice or by Bob) implies dephasing.

The state of B , accordingly commonly accepted interpretation, changes instantaneously at the moment of Alice joint AC measurement. But accordingly time reversal formalism developed by Laforest, Baugh and Laflamme (LBL) and the corresponding experiments [18, 25] the B “knows” about future AB measurement from very beginning. We aim to clear up this question with causal analysis. We will do it in the framework of usual tensor product treatment and LBL-like time reversal treatment.

5.1. Tensor product treatment

The peculiarity of our approach is that we consider Alice joint AC measurement as dephasing of degree p accordingly to Eq. (12). One may consider it as a soft measurement. More interesting consideration is that dephasing is a process from $p=0$ (measurement without record, that is pre-measurement) to $p=1$ (measurement is completed). Thus p is indirect time measure of this, certainly very fast process. The measurement which Bob may do to get to know something about his particle also is dephasing of a degree p_1 ; we will limit ourselves by the cases $p_1=0$ and $p_1=1$

So let the original matrix is:

$$\rho_{ABC}^0 = \rho_A \otimes \rho_{BC} = \rho_A \otimes |\Psi^-\rangle\langle\Psi^-|_{BC}, \quad (41)$$

Expand the matrix in Bell measurement basis:

$$\rho_{ABC}^0 = \sum_{i,j,k,l} F_{ijkl} |\Psi_i\rangle\langle\Psi_j|_{AC} \otimes |\phi_k\rangle\langle\phi_l|_B, \quad (42)$$

where $i, j=1,2,3,4$ correspond to the states (37), (38), (39) and (40) respectively; $k, l=1,2$ correspond to $|0\rangle_B, |1\rangle_B$ respectively; and $F_{ijkl} = \langle\Psi_i, \phi_k | \rho_{ABC}^0 | \Psi_j, \phi_l\rangle$.

Alice Bell measurement of AC means the replacement:

$$F_{ijkl} \rightarrow F_{ijkl}(1-p) \text{ at } i \neq j, \quad (43)$$

while Bob measurement of B means the replacement:

$$F_{ijkl} \rightarrow F_{ijkl}(1-p_1) \text{ at } k \neq l. \quad (44)$$

Transforming (42) according to (43) and (44), we obtain the resulting full matrix ρ_{ABC} (which explicit expression is very longish) and can do all the subsequent computation for causal analysis.

Consider the results for the simplest different variants of the input states A . A common property of all the variants described below turns out the fact, that in contradiction with classical intuition, there are no causal connections between any one-particle parties, in particular, $A \rightarrow B$. It is a simple consequence of the no-cloning theorem. Another common property is identity of causality in the partitions $AC-B$ and $AB-C$. So, below we concentrate on the partition $AC-B$.

1. A is in the definite state: $\rho_A = |0\rangle\langle 0|$. Figure 13 demonstrates qualitative quite expectable result. At $p=0$ causality is absent ($c_2(AC, B) = \infty$) as the state ABC is pure. At finite p causality $AC \rightarrow B$ appears that if information goes from Alice to Bob. It is natural that at $p_1=1$ causality is stronger since dephased B is more definite. When Alice completes her measurement ($p=1$), causality is most expressed: $c_2(AC, B)=1$ at any p_1 because B is already dephased together with C .

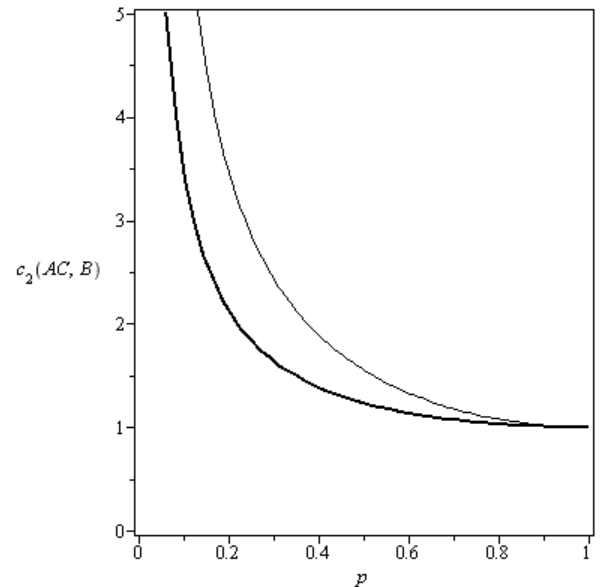


FIGURE 13. Causality at teleportation of $\rho_A = |0\rangle\langle 0|$ at $p_1=0$ (thin line) and $p_1=1$ (bold line).

2. A is in the maximally mixed state: $\rho_A = 1/2(|0\rangle\langle 0| + |1\rangle\langle 1|)$. Figure 14 demonstrates

stronger causality than in above case. The original ABC is mixed therefore the course of time is finite at $p=0$ already: $c_2(AC, B)=2$ at $p_1=0$ and $c_2(AC, B)=1$ at $p_1=1$. At $p \rightarrow 1$ causality amplifies to the utmost value: $c_2(AC, B) \rightarrow 0$ (that means the random input completely tends to determine a certain output, while recovery of input by output tends to full impossibility).

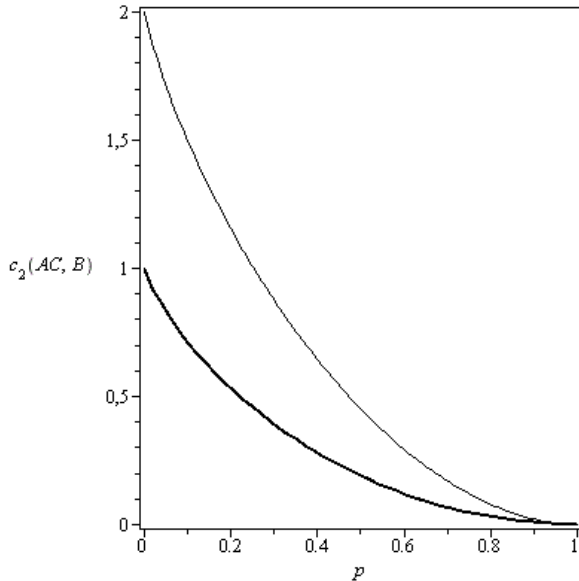


FIGURE 14. Causality at teleportation of $\rho_A = \frac{1}{2}(|0\rangle\langle 0| + |1\rangle\langle 1|)$ at $p_1=0$ (thin line) and $p_1=1$ (bold line).

3. A is in the pure equilibrium state: $\rho_A = 1/2(|0\rangle\langle 0| + |0\rangle\langle 1| + |1\rangle\langle 0| + |1\rangle\langle 1|)$. Figure 15 demonstrates that again at $p=0$ $c_2(AB, C) = \infty$ as the state ABC is pure. But as $p \rightarrow 1$ causality is different at different p_1 : $c_2(AC, B)=1$ at $p_1=0$ and $c_2(AC, B) \rightarrow 0$ at $p_1=1$. The latter is a clear result of Bob measurement of output qubit which selects a definite state from the superposition.

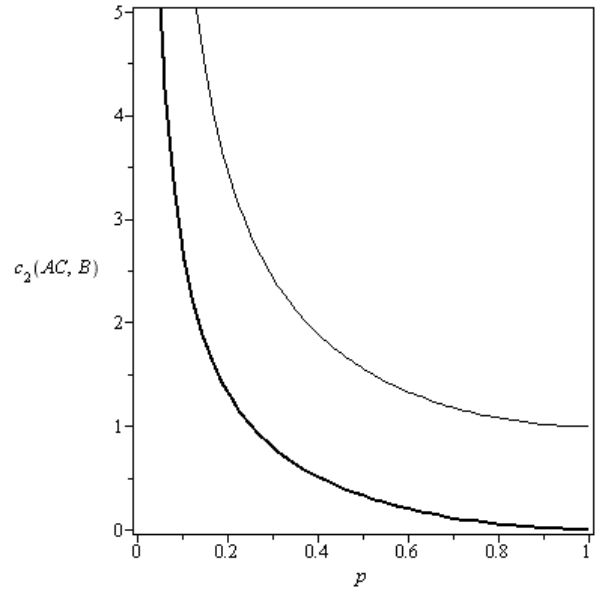


FIGURE 15. Causality at teleportation of $\rho_A = \frac{1}{2}(|0\rangle\langle 0| + |0\rangle\langle 1| + |1\rangle\langle 0| + |1\rangle\langle 1|)$ at $p_1=0$ (thin line) and $p_1=1$ (bold line).

Although qualitatively these formal results agree with intuition (namely Alice (AC) send quantum information to Bob (B)), note that any direction of time in the established causal link $AC \rightarrow B$ will do. Indeed, we nowhere specified when Bob measures (dephases) B . Bob's measurement may occur after Alice's measurement as well as *before*. Causality in reverse time is allowed. But "telegraph in the past" is impossible since a result of Alice's measurement is random. Instead Bob has the possibility of observation of the random future as existing reality. Next, we saw that Bob's measurement can only amplify the degree of causality $AC \rightarrow B$, but not generate it. That is the result of Bell measurement constitutes a cause with respect to every qubits of entangled pair just since moment of their birth (like [25]). There is no a contradiction with the above original statement: "the EPR source produces two entangled particles in the state (36)". This statement in fact is conditioned on absence of the future Bell measurement. Commonly accepted realizing of causality as directed only from the past to the future impeded to perceive that conditionality before.

5.2. Time reversal treatment

We follow LBL time reversal treatment described in detail in Ref. [18] with some simplification. The main idea is that Bell measurement and EPR source act as “time mirrors”. The input qubit (riding on the different particles as the carriers) travels to Alice’s Bell measurement device, reflects, travels backward in time to the EPR source, reflects and goes to Bob.

Every reflection is correspondent to some operator $W : |\psi\rangle^r = W_i |\psi\rangle$, where r is symbol of time reversal, the components $W_i^{a,b} = \langle b, a | \psi_i \rangle$ in Bell basis are: $W_1 = \mathbf{1}$, $W_2 = \sigma_z$, $W_3 = \sigma_x$, $W_4 = -i\sigma_y$. Qubit travel and transformations are shown in Fig. 16. The W_i means that we do not know results of Bell measurement; W_4 corresponds to our convention that the source generates the state (36).

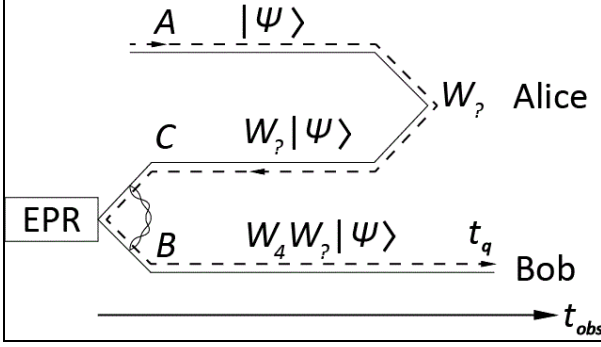


FIGURE 16. Time reversal treatment of teleportation from A to B ; t_{obs} is time of an external observer, t_q is proper time of the teleporting qubit.

It is not difficult to get the whole density matrix. But we are unable to implement gradual dephasing during Bell measurement. Instead we consider the most important practically both the extreme cases: measurement with ignoring of Bell measurement record (to compare with the case $p=0$ of tensor product treatment) and with taking into account the record (to compare with the case $p=1$ of tensor product treatment).

In the first case: (corresponding to $p=0$):

$$\rho_{ABC} = \frac{1}{4} \sum_{i=1}^4 |\psi, W_i \psi, W_4 W_i \psi\rangle \langle \psi, W_i \psi, W_4 W_i \psi|, \quad (45)$$

where $|\psi\rangle \langle \psi|$ is any input (A) state.

The second case (corresponding to $p=1$) is some more complicated, so we have restrict ourselves to the case of diagonal input states A that is $|\psi\rangle = |j\rangle \langle j|$,

$|j\rangle = |0\rangle, |1\rangle$. We introduce to the protocol a new object D which records the Bell measurement at Alice site. The state of D in Bell basis is $|\psi_i\rangle$ $i=1, 2, 3, 4$. As a result we have:

$$\rho_{ABCD} = \frac{1}{8} \sum_{j=1}^2 \sum_{i=1}^4 |j, W_i j, W_4 W_i j, \psi_i\rangle \langle j, W_i j, W_4 W_i j, \psi_i|. \quad (46)$$

We have computed all the c_2 (under condition $p_1=1$) with the following results.

In the first case: (corresponding to $p=0$) for A is in the definite state $c_2(AC, B) = \infty$; for A is in the maximally mixed state $c_2(AC, B) = 1$; A is in the pure equilibrium state $c_2(AC, B) = \infty$. Thus we have exactly the same result as in tensor product treatment.

In the second case (corresponding to $p=1$) we must take D instead of AB ($c_2(AC, B)$ are the same as in above case). For A is in the definite state $c_2(D, C) = 1$ that exactly the same as in tensor product treatment. If A is in the maximally mixed state $c_2(D, C)$ is indefinite (in tensor product treatment, having variable p we could take the limit at $p \rightarrow 1$: $c_2(AC, B) \rightarrow 0$).

Thus time reversal formalism gives in fact the same mathematical results as traditional tensor product one. But physically it proves our conclusion about causality in reverse time in much more strait manner. The random future D influences via backward time traveler C on the factual result of EPR emission.

With the recorder D we also can consider a partition $AD-B$ (which is equivalent of $AD-C$). As a result for A in the maximally mixed state we have $c_2(AD, B) = c_2(AD, C) = 1/2$. This value is minimal among all presented above finite values of c_2 , therefore causal connections $AD \rightarrow B$ and $AD \rightarrow C$ are the strongest ones. Since Bell measurement at Alice site occurred later (by time of an observer t_{obs}) than EPR emission took place, this result is further proof of causality in reverse time. The EPR pair “knows” about the random future – interaction with random A and random D . For A in the definite state $c_2(AD, B) = c_2(AD, C) = 1$. Therefore the greater is randomness of the future, the stronger is time reversal causality. Obviously in the case of deterministic future time reversal causality must absent. It is just impossibility of “telegraph to the past”.

6. Conclusions

The quantum causal analysis is extension of the classical one; therefore it is extension of formalized intuitive understanding of causality. Indeed in the simple situations our formal results are not surprising, e.g. when dissipating particle proved to be an effect. But even in these cases our formal approach has an advantage over usual informal, intuitive one, because it provides the *quantitative* measure of causal connection. However in the Quantum World common intuition often fails in rather simple systems, consisting of a few particles. Causal analysis quite works with any system, although its results may seem contrintuitively. Therewith these results turns out practically useful, e.g. in explanation of peculiarities of entanglement decay under different kind of decoherence or in relation between intersystem causality and consequences of asymmetric decoherence.

Very simple and general property of quantum causality is that it can be finite only in the mixed states. In our previous works [9-13] we interpreted this fact as quantum causality can be finite only in the open systems. But in the model of atom-field interaction considered in this paper the system is closed, the state mixedness, necessary for causality, was created before, at the stage of thermal state preparation. Therefore we have to correct interpretation as follows: *quantum causality can be finite only in the systems, which are or were open.*

The most prominent property of quantum causality is that it can exist in direct as well as *in reverse time*. Remarkably time reversal causality does not imply the naive classical paradoxes. We have considered such unusual causality in connection with contemporary teleportation experiments [18, 24, 25]. But, of course its significance is much wide, e.g. for interpretation and development of the forecasting experiments based on macroscopic entanglement [7, 8].

Acknowledgment

This work was supported by RFBR (grant 12-05-00001).

REFERENCES

1. N. A. Kozyrev, "On the possibility of experimental investigation of the properties of time", in *Time in Science and Philosophy*, edited by J. Zeman, Prague: Academia, 1971, pp. 111-132.
2. S. M. Korotaev, *Geomagnetism and Aeronomy* **32**, 27 (1992).
3. S. M. Korotaev, *Geomagnetism and Aeronomy* **35**, 387 (1995).
4. S. M. Korotaev, V. O. Serdyuk, V. I. Nalivaiko, A. V. Novysh, S. P. Gaidash, Yu. V. Gorokhov, S. A. Pulnits and Kh. D. Kanonidi, *Phys. of Wave Phenomena* **11**, 46 (2003).
5. S. M. Korotaev, A. N. Morozov, V. O. Serdyuk, J. V. Gorohov and V. A. Machinin, *NeuroQuantology* **3**, 275 (2005).
6. S. M. Korotaev, *Int. J. of Computing Anticipatory Systems* **17**, 61 (2006).
7. S. M. Korotaev, V. O. Serdyuk and J. V. Gorohov, *Hadronic Journal* **30**, 39 (2007).
8. S. M. Korotaev and V. O. Serdyuk, *Int. J. of Computing Anticipatory Systems* **20**, 31 (2008).
9. S. M. Korotaev and E. O. Kiktenko, AIP Conference Proceedings **1316**, 295 (2010).
10. S. M. Korotaev, *Causality and Reversibility in Irreversible Time*, Scientific Research Publishing, 2011.
11. S. M. Korotaev and E. O. Kiktenko, "Causality in the entangled states" in *Physical Interpretation of Relativity Theory* edited by P Rowlands, Moscow, BMSTU PH, 2011, pp. 140-149.
12. E. O. Kiktenko and S. M. Korotaev, *Phys. Lett.* **A376**, 820 (2012).
13. S. M. Korotaev and E.O. Kiktenko, *Physica Scripta*. **85**, 055006 (2012).
14. J. G. Cramer, *Phys. Rev.* **D22**, 362 (1980).
15. K. Zyczkowski, P. Horodecki, M. Horodecki and R. Horodecki, *Phys. Rev.* **A65**, 012101 (2002).
16. A. Borras, A. R. Plastino, M. Casas and A. Plastino, *Phys. Rev.* **A78**, 052104 (2008).
17. A. S. Elitzur and S. Dolev "Is there more to T?," in *The Nature of Time: Geometry, Physics and Perception*, edited by R. Buccery, M. Saniga and W. M. Stuckey, Kluwer Academic Publishers, 2003, pp. 297-306.
18. M. Laforest, J. Baugh and R. Laflamme, *Phys. Rev.* **A73**, 032323 (2006).
19. V. Coffman, J. Kundu and W. K. Wootters, *Phys. Rev.* **A61**, 052306 (2000).
20. W. Dür, *Phys. Rev.* **A63**, 020303 (2001).
21. S. S. Jang, Y. W. Cheong, J. Kim and H. W. Lee, *Phys. Rev.* **A74**, 062112 (2006).
22. W. Song and Z.-B. Chen, *Phys. Rev. A* **76**, 014307 (2007).
23. S. Bose, I. Fuentes-Guridi, P. L. Knight and V. Vedral, *Phys. Rev. Lett.* **87**, 050401 (2001).

24. S. Lloyd, L. Maccone, R. Garcia-Patron, V. Giovannetti, Y. Shikano, S. Pirandola, L. A. Rozema, A. Darabi, Y. Soudagar, L. K. Shalm, and A. M. Steinberg, *Phys. Rev. Lett.* **106**, 040403 (2011).
25. X.-S. Ma, S. Zotter, J. Kofler, R. Ursin, T. Jennewien, Č. Brukner and A. Zeilinger, *Nature Physics* **8**, 479 (2012).